Ab initio prediction of low-temperature parts of the phase diagram for the *M*Sb-*M′*Sb (*M*, *M′* = Al, Ga, or In) and AlSb-GaSb-InSb systems

I. V. Pentin, J. C. Schön, and M. Jansen
Max-Planck Institut für Festköperforschung, Heisenbergstr. 1, D-70569 Stuttgart, Germany
(Received 2 June 2010; revised manuscript received 3 September 2010; published 7 October 2010)

The low-temperature parts of phase diagrams for the quasibinary and quasiternary semiconductors of $A^{III}B^{V}$ type in the Al/Ga/In/Sb system were calculated based on the *ab initio* calculations without employing any experimental information. Via global exploration of the enthalpy landscapes for many different compositions in these systems, candidates for crystalline solid-solution phases were identified. Next, their free enthalpies were computed on *ab initio* level and the respective low-temperature phase diagram was derived. The miscibility gap of the quasiternary system was calculated based not only on the data of the corresponding binaries but also on additional information about enthalpies of formation of quasiternary compositions.

DOI: 10.1103/PhysRevB.82.144102 PACS number(s): 64.75.Qr, 81.30.Dz

I. INTRODUCTION

Knowing the thermodynamically stable phases of chemical compounds as a function of state variables (T,p,x_i) is of fundamental importance for many fields in science and technology. This information is conventionally encoded in equilibrium phase diagrams, which are descriptive in nature and need to be determined experimentally. Missing information, e.g., an omitted thermodynamically stable compound is inevitably detrimental to the reliability of this tool in practical materials science. But mapping the phase diagram via experiments at low temperatures is quite difficult since it is often nearly impossible to access the thermodynamic equilibrium due to the low speed of the solid-state reactions. The rather successful CALPHAD (Ref. 1) approach is hardly suitable to overcome this dilemma since it only allows to interpolate or extrapolate the experimental data available.

One way people have chosen to address this problem is the use of the cluster expansion method (or some variation thereof) combined with the quasichemical approximation.[2–4] Here, one assumes, that the alloy can be modeled as an ensemble of clusters individually independent statistically and energetically of the surrounding atomic configuration. That allows one to relatively quickly calculate the total free energy of a large set of configurations and to compute thermodynamic properties and as a result to construct the miscibility gap. Another approach is to use the valence-force-field model,[5–7] where one employs as input elastic constants measured experimentally or calculated theoretically, to calculate the formation energy of an alloy (for a review of the field see, e.g., Ref. 8). However, these approaches do not address the fundamental problem of identifying the thermodynamically stable phases in the system, not to speak of possible metastable modifications. In many instances, this may be justified because there is sufficient experimental evidence to unambiguously identify the thermodynamically stable phases. Thus, with the underlying lattice known, we can compute the phase diagram of, e.g., a solid solution via atomic decoration of the underlying lattice. But there exist many examples, where the thermodynamically stable phases of mixed compounds exhibit a very different structure from the one of the pure compounds[9,10] that cannot be derived by a simple relaxation from the (decorated) starting lattice. Thus, a systematic approach to the prediction of phase diagrams requires the identification of all thermodynamically stable phases in the system and their lattices.

In this work, we demonstrate at the example of the quasibinary and quasiternary (Al, Ga, In) antimonides, how the low-temperature part of their phase diagrams can be predicted without any input from experiment, via an unbiased global exploration of the energy landscapes of these systems combined with the computation of the Gibbs free energy on *ab initio* level. In particular, the calculation of the quasiternary phase diagram at low temperature is based not only on information about the quasibinaries but also includes additional data drawn from the landscape of the quasiternary system. This constitutes an important step beyond the usual procedure of generating the quasiternary phase diagram by extrapolation from the three quasibinary ones.

The semiconductor $A^{III}B^{V}$ systems are of great importance both in basic science research and in technological applications. Thus, the phase diagrams of the corresponding ternary nitrides,[11,12] phosphides,[13,14] arsenides,[13,15] and antimonides[13,16] have been investigated, since they provide information regarding the crystal growing process, and the stability of the material at working conditions. In particular, the antimonide based $A^{III}B^{V}$ semiconductor compounds have received much attention because of their applications in materials science and engineering,[17] e.g., for infrared optoelectronic devices.[18,19] A number of studies have been reported on the liquid-solid phase equilibria in *M*Sb-*M′*Sb, where *M*, *M′* = Al, Ga, or In (Refs. 20–30) since such information plays a key role in the growth of antimonide semiconductor crystals by liquid phase epitaxy. However, experimental thermodynamic data regarding the low-temperature part of their phase diagrams commonly assumed to exhibit a miscibility gap do not exist, especially for the quasiternary system. Nevertheless, this region of the phase diagram is no less important than the high-temperature part because the location of the miscibility gap informs the thermodynamic conditions, at which the final materials and products can be used without risking a failure due to the decomposition of the solid solution at low temperatures, e.g., room temperature T_R.

Thermodynamic modeling has been called upon for a long time to supplement experiment in deriving phase diagrams[1,8] and there are several studies in the literature addressing the

liquidus-solidus equilibria and miscibility gaps for the quasibinary systems MSb-M'Sb (M, M'=Al,Ga,In).[16,31–34] In Ref. 28 the two-sublattice model was used to describe the solidus curve in the AlSb-InSb system, and in Refs. 31 and 32 the regular solution model was applied to the solid phase in the quasibinary AlSb-GaSb and AlSb-InSb systems. Jianrong and Watson[16] improved the regular solution model by adding temperature-dependent variables to describe the GaSb-InSb system, and Ishida *et al.*[35] constructed the quasiternary phase diagram by extrapolating from the three quasibinary ones.

In all of these studies, the miscibility gaps were predicted via the extrapolation of thermodynamic functions, obtained at temperatures close to the liquid-solid equilibrium, to the low-temperature regions. However, these extrapolations are not satisfactory for several reasons. First, the models have been fitted to the experimental solidus and liquidus curves, but not to the thermodynamic potentials of the solid phase, such as heat-capacity data or the chemical potential. Second, one employs very simple models for the solidus curve (ideal or regular solution) while the nonideal behavior of the system is taken into account only by the model of the liquid phase. Third, one does not take into consideration that the variations in the heat capacities with temperature may cause crucial changes in the critical parameters, especially when extrapolating from high temperatures. Fourth, deducing the miscibility gap of the quasiternary system by extrapolating from the quasibinary ones is highly problematic since then by construction the maximum of the gap must lie on the boundary of the phase diagram. Finally, no information about possible ordered crystalline phases is included. As a consequence, the critical parameters derived are not satisfactory and are spread over a range of several hundred degrees. As will be demonstrated using the unbiased approach described below, the extrapolated miscibility gaps can differ by 200 K from the ones based on the *ab initio* calculations, and the low-temperature phase diagram of the quasiternary system is not only quantitatively but also qualitatively incorrect.

Recently, we have developed a general strategy to predict and compute phase diagrams in the low-temperature regime including both crystalline and solid-solution phases without recourse to any experimental information such as underlying lattices.[36,37] This approach employs a combination of global explorations of the energy landscape of the system[38] for many different compositions, using empirical potentials, and local optimizations of the structure candidates determined, on the *ab initio* level.

In the methods, Sec. II, we present a description of our approach, which includes several parts: a general description of the methodology (Sec. II A), details of *ab initio* calculations, and the global exploration procedure (Sec. II B) followed by details of calculation of the enthalpy of formation (Sec. II C) and the construction of the phase diagrams (Sec. II D). The results are presented in Sec. III, including the fit parameters derived for the miscibility gaps. Subsequently, the calculated data are interpreted and discussed in Sec. IV.

II. METHODS

A. General approach

Our general approach to the determination of structure candidates has been given in detail elsewhere[38,39] and our methodology for the study of the low-temperature region of phase diagrams is described in Ref. 37. Here we just outline the main steps of the method. The (meta)stable phases capable of existence correspond to locally ergodic regions on the enthalpy landscape of the chemical system under investigation. At low temperatures, these regions are basins around local minima of the potential energy while at elevated temperatures locally ergodic regions can encompass many (often structurally related) local minima. A prominent example of the latter case is the many disordered atom arrangements that contribute to a disordered alloy or solid-solution phase.

Finding these regions requires the use of a global optimization method to identify local minima, as well as a local optimization procedure for the subsequent refinement at an *ab initio* level. For the global search, we permit free variation in the atom positions and cell parameters, keeping the ionic charges fixed, where the energy is computed using an empirical potential. These global searches are performed for many different compositions in the given chemical system and several numbers of formula units Z in the simulation cell. Note that one is interested not only in the thermodynamically stable phases but also in as many of the metastable ones as possible. After a structure candidate has been found, it is locally optimized at an *ab initio* level. If many local minima exhibit the same cation-anion superstructure, we generate additional ternary structures belonging to the same superstructure, and locally optimize them at an *ab initio* level. One should note that this general procedure does not rely on any underlying lattice or any information regarding the existence or nonexistence of ordered crystalline compounds or solid solutions in the chemical system. By analyzing the large set of local minima found, we can identify possible crystalline or solid-solution phases. In a second step, we compute their free energies and determine the thermodynamically stable ones.

For the comparison of the cation-anion arrangements of the various structure candidates we employ the algorithm CMPZ (CoMPare Zell=compare cell),[40] implemented in the program KPLOT,[41] in order to identify possible structure families that would indicate the existence of, e.g., solid-solution phases. If all the structures belonging to the same superstructure exhibit essentially the same energy, we treat them as being part of the same locally ergodic region and compute the local free energy of this region. From this, we can then calculate the excess free enthalpy (Gibbs free energy) as a function of composition and temperature, and deduce the existence or nonexistence of a miscibility gap in the system. If no solid-solution phase is found, we employ the convex-hull method for the enthalpy of formation of the various stoichiometric crystalline phases, in order to identify the thermodynamically stable phases at 0 K.

B. *Ab initio* calculations and global exploration: Technical details

For the *ab initio* energy calculations we employ the program CRYSTAL 2006.[42] Here, we use a heuristic algorithm described in detail in Refs. 43 and 44, which is based on a nested sequence of line search minimizations. Finally, the

TABLE I. Ionic radii of atoms $r(q)$ ([Å]) and charges q used in the present work for the global landscape explorations of the semiconductor $A^{III}B^{V}$ systems.

	Al	Ga	In	Sb
q	+3	+3	+3	−3
$r(q)$	0.57	0.62	0.8	2.4

energy as function of the volume $E(V)$ is obtained by interpolation of the calculated data points with the standard Murnaghan formula.[45]

In this work, all calculations were performed on both the Hartree-Fock (HF) and density-functional theory (DFT) level. For the DFT calculations the Becke's three parameter functional[46] (B3LYP) and local density approximation von Barth-Hedin (LDA-VBH) functionals were employed. The basis sets were taken from the literature.[47]

The empirical potential employed during the global search for local minima consisted of a damped Coulomb term plus a Lennard-Jones-type potential, where the Lennard-Jones parameters $\sigma_{ij}=r_i+r_j$ are given by the sum of the ionic radii of atoms i and j with charge q_i and q_j (see Table I). As a global optimization algorithm, stochastic simulated annealing[48,49] runs based on random Monte Carlo walks on the energy landscape with decreasing temperature parameter were used, for each fixed composition with up to 20 atoms/simulation cell. Both atom positions (85% of all Monte Carlo steps) and the parameters of the periodically repeated simulation cell (15% of all Monte Carlo steps) were freely varied during the random walks. The supercells generated contained up to 32 atoms for quasibinary and up to 40 atoms for quasiternary systems, the limitation being the computational expense of the *ab initio* local optimization of cell parameters and atom positions.

C. Computation of the enthalpy of formation

After the energies of the local minima for structure candidates that belong to the solid-solution-like phase have been obtained, it is possible to calculate the enthalpy of formation of a compound A_xB_{1-x} by the following formula:

$$\Delta_f H(M_{1-x}M'_x\mathrm{Sb}) = \langle E(M_{1-x}M'_x\mathrm{Sb})\rangle - (1-x)E(M\mathrm{Sb}) - xE(M'\mathrm{Sb}), \quad (1)$$

where $\langle E(M_{1-x}M'_x\mathrm{Sb})\rangle$ is the average energy of the structure candidates belonging to the sphalerite structure family, $E(M\mathrm{Sb})$ and $E(M'\mathrm{Sb})$ are the energies of the boundary compounds MSb and M'Sb, respectively, and x is the fraction of M'Sb in the overall composition (M, M'=Al, Ga, or In). We note that for nonzero pressure, there should also be a term $p[\langle V(A_xB_{1-x})\rangle - xV(A) - (1-x)V(B)]$, where $V(A_xB_{1-x})$, $V(A)$, and $V(B)$ are the molar volumes of the minima contributing to the solid-solution state and of the pure compounds, respectively. However, the contribution of this term to the overall energy balance is usually too small to have a significant influence at standard pressures.

Obviously, this procedure yields a finite number of data points for different values of x and the Redlich-Kister polynomial[50] was used to fit the results,

$$\Delta_f H(x) = x(1-x)\sum_{i=0}^{N} a_i(1-2x)^i, \quad (2)$$

where a_i are the fitting parameters. Usually, one only considers the first couple of terms in the polynomial expansion since the total number of data points would not justify the use of higher-order polynomials.

Of course, if the compound A_xB_{1-x} is an ordered crystalline compound, only one minimum contributes to the locally ergodic region, and the energy average trivially equals the energy $E(A_xB_{1-x})$. Furthermore, these data points should be treated individually and it is usually not appropriate to try to fit $\Delta_f H(x)$ with some kind of polynomial function, the energies of such ordered structures do not change smoothly as a function of x since these structures are usually not simply related to each other.

D. Construction of the phase diagram

As mentioned above, the Gibbs energy of formation with respect to the pure compounds ($x=0$ and $x=1$) is then calculated by adding the standard entropy of mixing $S_{mix}(x) = -R[x\ln(x)+(1-x)\ln(1-x)]$,

$$\Delta_f G(x) = RT[x\ln(x)+(1-x)\ln(1-x)] + x(1-x)\sum_{i=0}^{N} a_i(1-2x)^i, \quad (3)$$

where $R=8.31451[\mathrm{J/(mol\ K)}]$ is the universal gas constant. (Of course, if we are dealing with an ordered compound A_xB_{1-x}, only one minimum contributes and the additional entropy term equals zero.) From $\Delta_f G(x)$, the phase diagram

TABLE II. The Redlich-Kister polynomial fitting parameters of the enthalpy of formation [according to Eq. (1)] for solid-solution phases in the MSb-M'Sb systems (M, M'=Al, Ga, or In) at standard pressure obtained in the present work (in joule).

	HF		DFT-B3LYP		DFT-LDA-VBH	
System	a_0	a_1	a_0	a_1	a_0	a_1
AlSb-GaSb	1764.1	45.1	2964.6	16.6	3472	61.2
AlSb-InSb	5866.4	−139.1	5756.2	113.2	5627.7	−1.3
GaSb-InSb	4185.5	84.5	4427.6	−140.8	4434.2	39.9

TABLE III. The critical parameters for the MSb-M'Sb systems (M, M'=Al, Ga, or In) systems at standard pressure obtained in the present work. T_c is the critical temperature of the decomposition in K and x_c is the concentration of the second compound. The literature data (x_c^{lit} and T_c^{lit}) are based on extrapolation from the liquidus-solidus region.

	HF		DFT-B3LYP		DFT-LDA-VBH		Literature data		
System	x_c	T_c	x_c	T_c	x_c	T_c	x_c^{lit}	T_c^{lit}	Ref.
AlSb-GaSb	0.48	106	0.5	178	0.49	209	0.5	207	31
AlSb-InSb	0.52	353	0.49	346	0.5	338	0.5	217, 180	28 and 32
GaSb-InSb	0.49	252	0.52	267	0.49	267	0.5	466	16

can now be obtained by means of the so-called convex-hull method[51] since the thermodynamically preferred combination of phases corresponds to linear combinations of appropriately chosen boundary phases with fractions $x_1, x_2, \ldots,$ of A that minimize the total Gibbs energy of the system. We note that as long as $\Delta_f H(A_x B_{1-x})$ can be described by a sufficiently low-order Redlich-Kister polynomial, there will never be more than two boundary phases for a given value of x. Furthermore, since $\lim_{x\to 0} \partial \Delta_f G(x)/\partial x = -\infty$ and $\lim_{x\to 1} \partial \Delta_f G(x)/\partial x = +\infty$, these boundary phases will never occur at $x=0$ or $x=1$ for nonzero temperature.

III. RESULTS

For each chemical system, several hundred global optimization runs (using simulated annealing) were performed for a number of different compositions each, at a pressure of 0 Pa. We performed calculations for five different compositions (3:1, 2:1, 1:1, 1:2, and 1:3) besides the limiting binary phases for all three MSb-M'Sb systems (M, M'=Al, Ga, or In) and for ten different compositions (1:1:1, 1:1:2, 1:2:1, 2:1:1, 1:2:2, 2:1:2, 2:2:1, 1:1:3, 1:3:1, and 3:1:1) for the quasiternary system. For each composition, we found for the set of structure candidates with the lowest energies, that the energy differences between the candidates were very small (compared to $k_B T_R$). Furthermore, these candidates belonged to the same structure family (cations and anions arranged according to the sphalerite type in agreement with experimental observation[13]), indicating a solid-solution behavior for the three quasibinary and the quasiternary systems. To explore the energy landscape of all four systems in more detail, a number of structure candidates belonging to the sphalerite structure family were generated by permutation of the cation positions followed by two local optimization runs: first with the empirical potential and subsequently on *ab initio* level. As a next step, we calculated the enthalpy of formation in the three quasibinary systems for each composition x according to formula (1). The parameters for a fit of $\Delta_f H(x)$ with a Redlich-Kister polynomial for all of the quasibinary systems are listed in Table II. From this data we calculated Gibbs energies according to formula (3) of the solid phase and predicted the location of the miscibility gaps. The critical parameters are listed in Table III. In Figs. 1–3 the predicted binodal curves for HF and DFT (with functionals B3LYP and LDA-VBH) based calculations and plots of the miscibility gaps based on literature data are shown. As a next step, we calculated the enthalpies of formation for the quasiternary system for each composition xb and xc by the following formula:

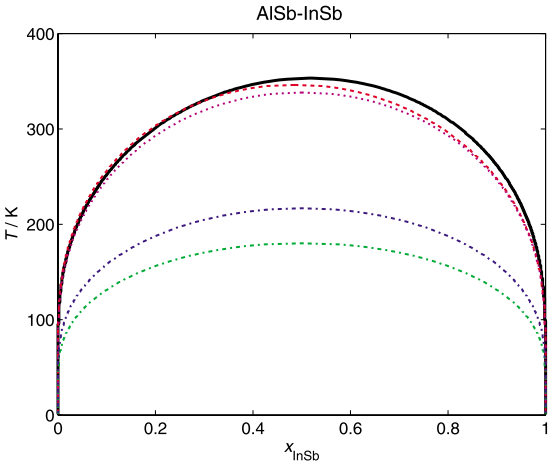

FIG. 1. (Color online) The miscibility gap in the AlSb-InSb system. Black solid curve based on HF calculations, red dashed curve based on DFT-B3LYP calculations, magenta dotted curve based on DFT-LDA-VBH calculations, blue (upper) and green (lower) dashed-dotted curve based on the extrapolated data from liquid/solid equilibria, (Refs. 28 and 32) respectively.

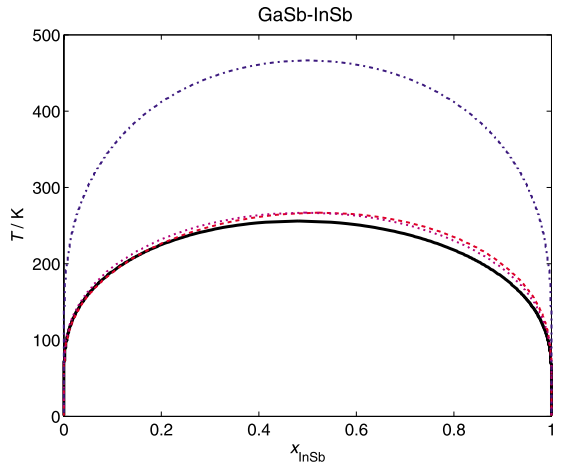

FIG. 2. (Color online) The miscibility gap in the GaSb-InSb system. Black solid curve based on HF calculations, red dashed curve based on DFT-B3LYP calculations, magenta dotted curve based on DFT-LDA-VBH calculations, blue dashed-dotted curve based on the extrapolated data from liquid/solid equilibria (Ref. 16).

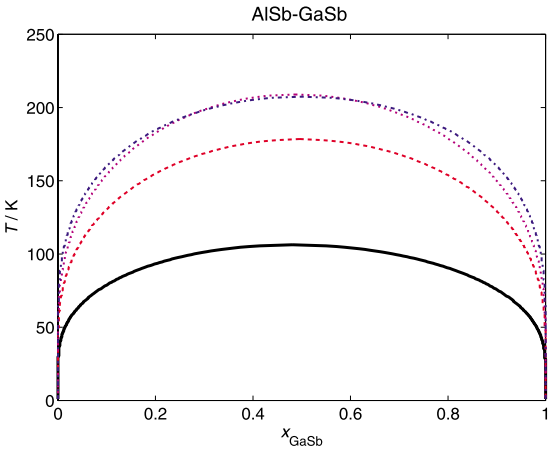

FIG. 3. (Color online) The miscibility gap in the AlSb-GaSb system. Black solid curve based on HF calculations, red dashed curve based on DFT-B3LYP calculations, magenta dotted curve based on DFT-LDA-VBH calculations, blue dashed-dotted curve based on the extrapolated data from liquid/solid equilibria (Ref. 31).

$$\Delta_f H(\mathrm{Al}_{1-xb-xc}\mathrm{Ga}_{xb}\mathrm{In}_{xc}\mathrm{Sb}) = \langle E(\mathrm{Al}_{1-xb-xc}\mathrm{Ga}_{xb}\mathrm{In}_{xc}\mathrm{Sb})\rangle - (1-xb-xc)E(\mathrm{AlSb}) - xbE(\mathrm{GaSb}) - xcE(\mathrm{InSb}), \quad (4)$$

where $\langle E(\mathrm{Al}_{1-xb-xc}\mathrm{Ga}_{xb}\mathrm{In}_{xc}\mathrm{Sb})\rangle$ is the average energy of the structure candidates belonging to the sphalerite structure family, E(AlSb), E(GaSb), and E(InSb) are the energies of the boundary compounds AlSb, GaSb, and InSb, respectively, xb is the fraction of GaSb and xc is the fraction of InSb in the overall composition. The parameters for a fit of the excess Gibbs energy for the quasiternary system are listed in Table IV. From this data we calculated Gibbs energies of the solid phase using a Redlich-Kister model and predicted the location of the miscibility gaps according to the following formula:

$$\Delta G^{sol} = \Delta_f H_{\mathrm{AlSb\text{-}InSb}} + \Delta_f H_{\mathrm{AlSb\text{-}GaSb}} + \Delta_f H_{\mathrm{GaSb\text{-}InSb}} - TS_{mix} + x_{\mathrm{AlSb}}x_{\mathrm{GaSb}}x_{\mathrm{InSb}}\sum_{i=1}^{3} x_i L_i, \quad (5)$$

where $\Delta_f H_{M\mathrm{Sb}\text{–}M'\mathrm{Sb}}$ are the enthalpies of formation of the quasibinary systems (M, M'=Al, Ga, or In), obtained earlier in the present work [according to Eq. (1)]; $L_i \triangleq$ fitting parameters (see Table IV); $S_{mix} \triangleq$ ideal entropy of mixing. Figure 4 depicts the isothermal sections of the predicted binodal curves (HF-based calculations) of the phase diagram for the AlSb-GaSb-InSb system at temperatures 250 K, 350 K, 450 K, 520 K, and 570 K, respectively, clearly showing the maximum of the miscibility gap inside the ternary region. The same behavior was observed with both DFT methods.

TABLE IV. The fitting parameters of the enthalpy of formation [according to Eq. (5)] for solid-solution phases in the AlSb-GaSb-InSb systems at standard pressure obtained in the present work (in joule).

Parameters	HF	DFT-B3LYP	DFT-LDA-VBH
L1	6870	11352	−236
L2	−6465	−7577	−2672
L3	39646	19952	15185

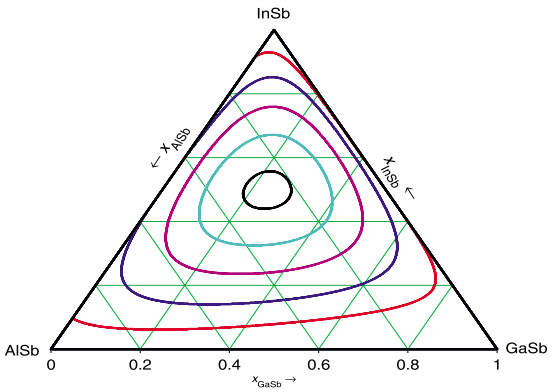

FIG. 4. (Color online) The five isothermal projections of the phase diagram for the AlSb-GaSb-InSb system at 250, 350, 450, 520, and 570 K, based on the HF calculations. Red curve −250 K, blue curve −350 K, magenta curve −450 K, cyan curve −520 K, and black curve −570 K.

IV. DISCUSSION AND CONCLUSION

In this study, we have found that all quasibinary antimonides exhibit a thermodynamically stable solid-solution-like phase at low temperatures, regardless of whether the energy was calculated on a HF or DFT (both with B3LYP and LDA-VBH functionals) basis. Figures 1–3 depict quite good agreement between all three, i.e., HF (black curve), DFT-B3LYP (red curve), and DFT-LDA-VBH (magenta curve), calculations. Since it is difficult to choose the most accurate *ab initio* method to calculate enthalpies of formation without experimental data about the system, using different methods gives a feeling for the quantitative validity of the results and the limits of the miscibility gap location. In spite of an apparently big difference between the HF and the DFT calculations for AlSb-GaSb, it is, nevertheless, within the expected range of errors: in earlier work, we have estimated the range of error in the location of the miscibility gap for different *ab initio* methods as 50–100 K.[37] Thus, we can expect, that for the AlSb-GaSb system the miscibility gap curves obtained via HF and DFT indicate the limits of the actual miscibility gap location in this system.

In contrast, the miscibility gaps extrapolated from high-temperature data for AlSb-InSb and GaSb-InAb differ by about 200 K from the gaps based on *ab initio* calculations. In Sec. I, we have already mentioned, that no direct experimental data exist for the miscibility gaps. Thus, the results we have obtained appear to be more convincing for the AlSb-InSb and GaSb-InAb systems, than extrapolations from high temperatures since all three *ab initio* methods give essentially the same result.

The same behavior was observed in the calculations for the quasiternary system AlSb-GaSb-InSb: no thermodynamically stable ordered compounds exist, and the low-

temperature phase diagram exhibits a dome-shaped miscibility gap with a maximum inside the ternary region, irrespective of whether the enthalpies of formation of the quasiternary compounds were computed on HF or DFT basis. This is in stark contrast to the results obtained from extrapolating only the quasibinary data,[35] where the maximum of the gap is located on the GaSb-InSb boundary. Clearly, the extrapolated phase diagrams currently available for the technologically important quasibinary and quasiternary mixed semiconductor systems MSb-M'Sb (M, M' = Al, Ga, In) and AlSb-GaSb-InSb, respectively, are not really satisfactory.

However, as we have demonstrated in this study, combining the global exploration of the whole quasiternary energy landscape with the calculation of enthalpies and free energies of formation on *ab initio* level for the ordered and solid-solution compounds determined during this search, allows us to address this problem and both predict and compute the low-temperature part of phase diagrams. This general approach also yields the answer to the fundamental (and often ignored) question, whether the thermodynamically stable phases of a particular system are ordered compounds or solid solutions, without needing any input from experimental data.

[1] A. M. N. Saunders, *CALPHAD: A Comprehensive Guide* (Pergamon, Oxford, 1998).
[2] L. K. Teles, J. Furthmüller, L. M. R. Scolfaro, J. R. Leite, and F. Bechstedt, Phys. Rev. B **62**, 2475 (2000).
[3] C. Caetano, L. K. Teles, M. Marques, A. Dal Pino, Jr., and L. G. Ferreira, Phys. Rev. B **74**, 045215 (2006).
[4] J. Z. Liu and A. Zunger, Phys. Rev. B **77**, 205201 (2008).
[5] I.-h. Ho and G. B. Stringfellow, Appl. Phys. Lett. **69**, 2701 (1996).
[6] T. Saito and Y. Arakawa, Phys. Rev. B **60**, 1701 (1999).
[7] K. Biswas, A. Franceschetti, and S. Lany, Phys. Rev. B **78**, 085212 (2008).
[8] J. C. Schön and M. Jansen, Int. J. Mater. Res. **100**, 135 (2009).
[9] I. V. Pentin, J. C. Schön, and M. Jansen, J. Chem. Phys. **126**, 124508 (2007).
[10] I. V. Pentin, J. C. Schön, and M. Jansen, Z. Anorg. Allg. Chem. **636**, 1703 (2010).
[11] B. Burton, A. van de Walle, and U. Kattner, J. Appl. Phys. **100**, 113528 (2006).
[12] C. K. Gan, Y. P. Feng, and D. J. Srolovitz, Phys. Rev. B **73**, 235214 (2006).
[13] M. B. Panish and M. Ilegems, Prog. Solid State Chem. **7**, 39 (1972).
[14] C. Li, J. Li, Z. Du, and W. Zhang, J. Phase Equilib. **21**, 357 (2000).
[15] I. V. Pentin, J. C. Schön, and M. Jansen, Phys. Chem. Chem. Phys. **12**, 8491 (2010).
[16] Y. Jianrong and A. Watson, CALPHAD: Comput. Coupling Phase Diagrams Thermochem. **18**, 165 (1994).
[17] B. R. Bennett, R. Magno, J. B. Boos, W. Kruppa, and M. G. Ancona, Solid-State Electron. **49**, 1875 (2005).
[18] J. Meyer, C. Hoffman, F. Bartoli, and L. Rammohan, Appl. Phys. Lett. **67**, 757 (1995).
[19] A. B. Djurišić, Y. Chan, and E. H. Li, Mater. Sci. Eng. R. **38**, 237 (2002).
[20] Z. Muszynski and N. G. Riabcev, J. Cryst. Growth **36**, 335 (1976).
[21] L. M. Foster, J. E. Scardefield, and J. F. Woods, J. Electrochem. Soc. **119**, 765 (1972).
[22] J. C. Woolley and B. A. Smith, Proc. Phys. Soc. London, Sect. B **70**, 153 (1957).
[23] J. C. Woolley and B. A. Smith, Proc. Phys. Soc. London **72**, 214 (1958).
[24] H. J. van Hook and E. S. Lenker, Trans. Metall. Soc. AIME **227**, 220 (1963).
[25] E. E. Matyas, Phys. Status Solidi A **42**, K129 (1977).
[26] J. F. Miller, H. L. Goering, and R. C. Himes, J. Electrochem. Soc. **107**, 527 (1960).
[27] R. L. Aulombard and A. Joullie, Mater. Res. Bull. **14**, 349 (1979).
[28] K. Ishida, T. Shumiya, H. Ohtani, M. Hasebe, and T. Nishizawa, J. Less-Common Met. **143**, 279 (1988).
[29] N. A. Goryunova, *The Chemistry of Diamond-Like Semiconductors* (MIT, Cambridge, 1965).
[30] G. B. Blom and T. S. Plaskett, J. Electrochem. Soc. **118**, 1831 (1971).
[31] R. C. Sharma and M. Srivastava, CALPHAD: Comput. Coupling Phase Diagrams Thermochem. **16**, 387 (1992).
[32] R. C. Sharma and M. Srivastava, CALPHAD: Comput. Coupling Phase Diagrams Thermochem. **16**, 409 (1992).
[33] L. Kaufman, J. Nell, K. Taylor, and F. Hayes, CALPHAD: Comput. Coupling Phase Diagrams Thermochem. **5**, 185 (1981).
[34] G. B. Stringfellow, J. Phys. Chem. Solids **33**, 665 (1972).
[35] K. Ishida, H. Tokunaga, H. Ohtani, and T. Nishizawa, J. Cryst. Growth **98**, 140 (1989).
[36] J. C. Schön and M. Jansen, in *Solid State Chemistry of Inorganic Materials V*, MRS Symposia Proceedings Vol. 848, edited by J. Li, N. E. Brese, M. G. Kanatzidis, and M. Jansen (Materials Research Society, Warrendale, 2005).
[37] J. C. Schön, I. V. Pentin, and M. Jansen, Phys. Chem. Chem. Phys. **8**, 1778 (2006).
[38] J. C. Schön and M. Jansen, Angew. Chem., Int. Ed. Engl. **35**, 1286 (1996).
[39] J. C. Schön and M. Jansen, Z. Kristallogr. **216**, 307 (2001).
[40] R. Hundt, J. C. Schön, and M. Jansen, J. Appl. Crystallogr. **39**, 6 (2006).
[41] R. Hundt, *KPLOT: A Program for Plotting and Investigation of Crystal Structures* (University of Bonn, Germany, 1979).
[42] V. R. Saunders, R. Dovesi, C. Roetti, M. Causa, N. M. Harrison, R. Orlando, and C. M. Zicovich-Wilson, *CRYSTAL 2006* (University of Torino, Torino, 2006).
[43] J. C. Schön, Ž. Čančarević, and M. Jansen, J. Chem. Phys. **121**, 2289 (2004).
[44] Ž. Čančarević, J. C. Schön, and M. Jansen, Mater. Sci. Forum **453**, 71 (2004).
[45] F. D. Murnaghan, Proc. Natl. Acad. Sci. U.S.A. **30**, 244 (1944).

[46] A. D. Becke, J. Chem. Phys. **98**, 5648 (1993).
[47] Available on website http://www.crystal.unito.it/Basi_Sets/ptable.html
[48] S. Kirkpatrick, C. D. Gelatt, Jr., and M. P. Vecchi, Science **220**, 671 (1983).
[49] V. Černý, J. Optim. Theory Appl. **45**, 41 (1985).
[50] O. Redlich and A. T. Kister, Ind. Eng. Chem. **40**, 345 (1948).
[51] G. Voronin, Russ. J. Phys. Chem. **77**, 1685 (2003).